

Multiband-OFDM MIMO Coding Framework for UWB Communication Systems

W. Pam Siritwongpairat, *Student Member, IEEE*, Weifeng Su, *Member, IEEE*, Masoud Olfat, *Member, IEEE*, and K. J. Ray Liu, *Fellow, IEEE*

Abstract—The emerging ultrawideband (UWB) system offers a great potential for the design of high speed short-range wireless communications. In order to satisfy the growing demand for higher data rates, one possible solution is to exploit both spatial and multipath diversities via the use of multiple-input multiple-output (MIMO) and proper coding techniques. In this paper, we propose a general framework to analyze the performance of multiband UWB-MIMO systems regardless of specific coding schemes. A combination of space-time-frequency (STF) coding and hopping multiband OFDM modulation is also proposed to fully exploit all of the available spatial and frequency diversities, richly inherent in UWB environments. We quantify the performance merits of the proposed scheme in case of Nakagami- m frequency-selective fading channels. Different from the conventional STF coded MIMO-OFDM system, the performance of the STF coded hopping multiband UWB does not depend on the temporal correlation of the propagation channel. We show that the maximum achievable diversity of multiband UWB-MIMO system is the product of the number of transmit and receive antennas, the number of multipath components, and the number of jointly encoded OFDM symbols. Interestingly, the diversity gain does not severely depend on the fading parameter m , and the diversity advantage obtained under Nakagami fading with arbitrary m parameter is almost the same as that obtained in Rayleigh fading channels. Finally, simulation results are presented to support the theoretical analysis.

Index Terms—Frequency selective fading channels, multiband orthogonal frequency-division multiplexing (OFDM), multiple antennas, space-time-frequency coding, ultrawideband (UWB), wireless personal area networks (WPANs).

I. INTRODUCTION

ULTRAWIDEBAND (UWB) is an emerging technology that offers great promises to satisfy the growing demand for low cost and high-speed digital wireless home networks.

Manuscript received December 21, 2004; revised March 26, 2005. This work was supported in part by the U.S. Army Research Laboratory under Cooperative Agreement DAAD 190120011. The associate editor coordinating the review of this manuscript and approving it for publication was Dr. Yuan-Pei Lin.

W. P. Siritwongpairat and K. J. R. Liu are with the Department of Electrical and Computer Engineering and Institute for Systems Research, University of Maryland, College Park, MD 20742 USA (e-mail: wipawee@eng.umd.edu; kjrlu@eng.umd.edu).

W. Su was with the Department of Electrical and Computer Engineering and Institute for Systems Research, University of Maryland, College Park, MD 20742 USA. He is now with the Department of Electrical Engineering, State University of New York (SUNY) at Buffalo, Buffalo, NY 14260 USA (e-mail: weifeng@eng.buffalo.edu).

M. Olfat was with the Department of Electrical and Computer Engineering and Institute for Systems Research, University of Maryland, College Park, MD 20742 USA. He is now with Nextel Communications, Inc. (e-mail: masoud.olfat@nextel.com).

Digital Object Identifier 10.1109/TSP.2005.861092

UWB is defined as any radio transmission that occupies a bandwidth of more than 20% of its center frequency, or nominally more than 500 MHz. In 1998, the Federal Communications Commission (FCC) has mandated that UWB radio transmission can legally operate in the range from 3.1 GHz to 10.6 GHz, at a transmit power of -41.3 dBm/MHz [1]. Depending on how the available bandwidth is utilized, UWB can be divided into two groups: single band and multiband.

A traditional UWB technology is based on single-band systems employing carrier-free communications [2]–[6]. It is implemented by directly modulating information into a sequence of impulse-like waveforms, which occupy the available bandwidth of 7.5 GHz. Multiple users can be supported via the use of time hopping or direct sequence spreading approaches. The single band system faces a challenging problem in building RF and analog circuits, and in designing a low complexity receiver that can capture sufficient multipath energy.

Recently, multiband UWB schemes were proposed in [7]–[9], in which the UWB frequency band is divided into several subbands. Each subband occupies a bandwidth of at least 500 MHz in compliance with the FCC regulations. By interleaving the symbols across subbands, multiband UWB can maintain the transmit power as if the large GHz bandwidth is utilized. The advantage is that multiband approach allows the information to be processed over a much smaller bandwidth, thereby reducing overall design complexity as well as improving spectral flexibility and worldwide compliance. To efficiently capture the multipath energy, orthogonal frequency division multiplexing (OFDM) technique has been used to modulate the information in each subband. The major difference between multiband OFDM and traditional OFDM schemes is that the multiband OFDM symbols are not continually sent on one frequency-band; instead, they are interleaved over different subbands across both time and frequency. Multiple access of multiband UWB is enabled by the use of suitably designed frequency-hopping sequences over the set of subbands.

Currently, UWB technology achieves data rates ranging from 55 to 480 Mb/s over distances up to 10 m. To enhance the data rates and the coverage ranges, the employment of multiple-input multiple-output (MIMO) scheme to UWB has gained considerable interest recently. In conventional RF technology, MIMO has been well known for its effectiveness of improving system performance in fading environments. Space-time (ST) coded MIMO systems [12]–[14] have been proposed for narrowband communications, where the fading channel is frequency-nonspecific. The main concept is the joint processing in time as well as in space via the use of multiple transmit and receive antennas, so as to achieve both

spatial and temporal diversities. When the fading channel is frequency-selective, space-frequency (SF) coded MIMO-OFDM systems [15]–[20] have been shown to be an efficient approach to make benefits of spatial and frequency diversities. Recently, space-time-frequency (STF) codes [21]–[23] have also been proposed for MIMO-OFDM systems. By utilizing some proper STF coding and modulation techniques, STF coded MIMO systems can exploit all of the spatial, temporal and frequency diversities, and hence promise to yield remarkable performance improvement.

Most UWB applications are in rich scattering indoor environment, which provides an ideal transmission scenario for MIMO implementation. In addition, the GHz center frequency of UWB radio relaxes the requirements on the spacing between antenna array elements. Consequently, the combination of UWB and MIMO technology will become a viable and cost-efficient method to achieve the very high data rate requirement for future short range wireless applications. To this date, multi-antenna UWB technology has been well documented for the traditional single-band UWB system [24]–[27]. On the other hand, research for multi-antenna multiband UWB systems is still largely unexplored, thus offering limited resources in handling the benefits and challenges of UWB-MIMO communications.

In this paper, we propose a general framework to characterize the performance of UWB-MIMO systems with multiband OFDM. A combination of STF coding and hopping multiband UWB transmission is proposed to exploit all of the available spatial and frequency diversities. In the performance evaluation, we do not impose any restriction on the delays or the average powers of the multipath components, and the proposed framework is applicable for any channel models. Several models have been used for UWB channel models, for example, tap-delay line Nakagami- m fading model [28], the modified Saleh-Valenzuela model [29], and the Δ -K model described in [30]. Since Nakagami- m statistics can be used to model a wide range of fading conditions, we evaluate the theoretical performances of UWB systems by using the tap-delay line Nakagami- m fading model, as it can provide some insightful understanding of UWB systems [5], [24]–[26], [31], [32]. We quantify the average pairwise error probability as well as the diversity and the coding advantages, regardless of specific coding schemes. It turns out that the maximum achievable diversity is the product of the number of transmit and receive antennas, the number of multipath components, and the number of jointly encoded OFDM symbols. An interesting result is that the diversity advantage does not depend on the fading parameter m . The diversity gain obtained under Nakagami fading with arbitrary m parameter is almost the same as that obtained in Rayleigh fading, which is equivalent to Nakagami- m fading with $m = 1$. Simulation results confirm the theoretical expectation of considerable performance improvement, gained from adopting STF codes in multiband system.

The rest of the paper is organized as follows. In Section II, we present the multiband UWB-MIMO system model, including the signal modulation, channel model, receiver description, and detection technique. The performance analysis of a peer-to-peer multi-antenna multiband UWB system is presented in Section III. Section IV shows simulation results, and finally Section V concludes the paper.

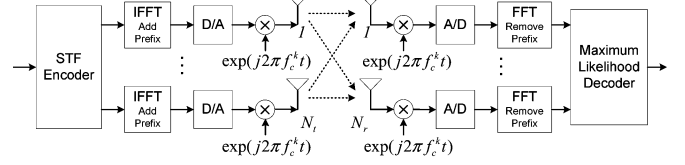


Fig. 1. Multiband UWB-MIMO system.

II. MULTIBAND UWB-MIMO SYSTEM MODEL

Consider a multiband OFDM scenario that has been proposed in the IEEE 802.15.3a WPAN standard [33]. The available UWB spectrum of 7.5 GHz is divided into several subbands, each with bandwidth BW of at least 500 MHz. Each user utilizes one subband per transmission. For each user, signals from all transmit antennas share the same subband. Within each subband, OFDM modulation with N subcarriers is used at each transmit antenna. Different bit rates are achieved by using different channel coding, frequency spreading, or time spreading rates. We consider a multiband UWB system with fast band-hopping rate, i.e., the signal is transmitted on a frequency-band during one OFDM symbol interval, then moved to a different frequency band at the next interval.

A. Transmitter Description

We consider a peer-to-peer multiband UWB system with N_t transmit and N_r receive antennas, as shown in Fig. 1. The information is encoded across N_t transmit antennas, N OFDM subcarriers, and K OFDM blocks.

At the transmitter, the coded information sequence from a channel encoder is partitioned into blocks of N_b bits. Each block is mapped onto a $KN \times N_t$ STF codeword matrix

$$\mathbf{D} = [\mathbf{D}_0^T \quad \mathbf{D}_1^T \quad \cdots \quad \mathbf{D}_{K-1}^T]^T \quad (1)$$

where

$$\mathbf{D}_k = [\mathbf{d}_1^k \quad \mathbf{d}_2^k \quad \cdots \quad \mathbf{d}_{N_t}^k], \quad (2)$$

in which $\mathbf{d}_i^k = [d_i^k(0)d_i^k(1)\cdots d_i^k(N-1)]^T$ for $i = 1, 2, \dots, N_t$ and $k = 0, 1, \dots, K-1$. The symbol $d_i^k(n)$, $n = 0, 1, \dots, N-1$, represents the complex symbol to be transmitted over subcarrier n by transmit antenna i during the k th OFDM symbol period. The matrix \mathbf{D} is normalized to have average energy $E[\|\mathbf{D}\|^2] = KN N_t$, where $E[\cdot]$ stands for the expectation operation, and $\|\cdot\|$ denotes the Frobenius norm [34]. At the k th OFDM block, the transmitter applies N -point IFFT over each column of the matrix \mathbf{D}_k , yielding an OFDM symbol of length T_{FFT} . In order to mitigate the effect of intersymbol interference, a cyclic prefix of length T_{CP} is added to the output of the IFFT processor.

After adding the cyclic prefix and guard interval, the OFDM symbol is passed through a digital-to-analog converter, resulting in an analog baseband OFDM signal of duration $T_{\text{SYM}} = T_{\text{FFT}} + T_{\text{CP}} + T_{\text{GI}}$, where T_{GI} denotes the guard interval duration. The baseband OFDM signal to be transmitted

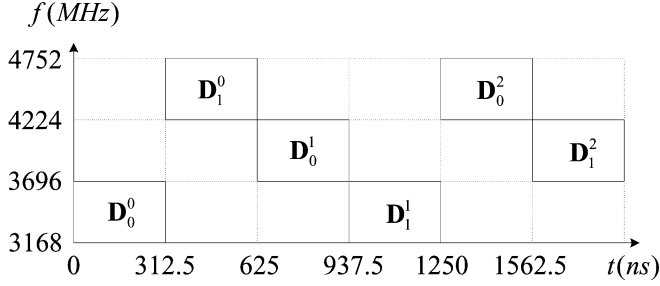


Fig. 2. Time-frequency representation of multiband UWB symbols with $K = 2$ and fast band-hopping rate.

by the i th transmit antenna at the k th OFDM block can be expressed as

$$x_i^k(t) = \sqrt{\frac{E}{N_t}} \sum_{n=0}^{N-1} d_i^k(n) \exp\{j2\pi n \Delta f (t - T_{CP})\}$$

where $t \in [T_{CP}, T_{FFT} + T_{CP}]$, $\mathbf{j} \triangleq \sqrt{-1}$, and $\Delta f = 1/T_{FFT}$ = BW/N is the frequency separation between two adjacent subcarriers. The factor $\sqrt{E/N_t}$ guarantees that the average energy per transmitted symbol is E , independent of the number of transmit antennas. In the interval $[0, T_{CP}]$, $x_i^k(t)$ is a copy of the last part of the OFDM symbol, and $x_i^k(t)$ is zero in the interval $[T_{FFT} + T_{CP}, T_{SYM}]$.

The complex baseband signal $x_i^k(t)$ is filtered, up-converted to an RF signal with a carrier frequency f_c^k , and finally sent from the i th transmit antenna. The transmitted multiband OFDM signal at transmit antenna i over K OFDM symbol periods is given by

$$s_i(t) = \sum_{k=0}^{K-1} \text{Re}\{x_i^k(t - kT_{SYM}) \exp(j2\pi f_c^k t)\},$$

where $\text{Re}\{x\}$ takes the real part of x . The carrier frequency f_c^k specifies the subband, in which the signal is transmitted during the k th OFDM symbol period. The carrier frequency can be changed from one OFDM block to another, so as to enable the frequency diversity while minimize the multiple access interference. The band hopping rate depends on the channel environment and the desired data rates. Since the signals from all transmit antennas share the same subband, f_c^k is identical for every transmit antenna. Note that the transmissions from all of the N_t transmit antennas are simultaneous and synchronous. Fig. 2 illustrates a time-frequency representation of the transmitted signal, which is based on a time-frequency code that has been proposed for the IEEE 802.15.3a standard [9]. In this example, the STF coding is performed across $K = 2$ consecutive OFDM blocks, and the superscript τ of \mathbf{D}_k^τ represents the index of STF codewords. Since N_b information bits are transmitted in KT_{SYM} seconds, the transmission rate (without channel coding) is $R = N_b/(KT_{SYM})$.

B. Channel Model

We consider a tap-delay line Nakagami- m fading channel model with L taps. At the k th OFDM block, the channel im-

pulse response from the i th transmit antenna to the j th receive antenna can be described as

$$h_{ij}^k(t) = \sum_{l=0}^{L-1} \alpha_{ij}^k(l) \delta(t - \tau_l) \quad (3)$$

where $\alpha_{ij}^k(l)$ is the multipath gain coefficient, L denotes the number of resolvable paths, and τ_l represents the path delay of the l th path. The measurements in UWB channels indicate that the amplitude of each path follows either a log-normal or Nakagami- m distribution [28], [29]. The Nakagami fading parameter, m , describes the severity of the fading. It can be any real value that satisfies $m \geq 1/2$. The smaller the m , the more severe the fading, with $m = 1$ and $m = \infty$ corresponding to the Rayleigh fading and nonfading channel, respectively. The advantage of Nakagami- m statistics is that they can model a wide range of fading conditions by adjusting their fading parameters. In fact, Nakagami- m distributions with large value m are similar to the log-normal distributions. Therefore, we will perform the theoretical analysis based on the Nakagami- m distribution. Specifically, the amplitude of the l th path, $|\alpha_{ij}^k(l)|$, is modeled as a Nakagami- m random variable with a probability density function (pdf) [35]

$$p_{|\alpha_{ij}^k(l)|}(x) = \frac{2}{\Gamma(m)} \left(\frac{m}{\Omega_l}\right)^m x^{2m-1} \exp\left(-\frac{m}{\Omega_l} x^2\right)$$

where $\Gamma(\cdot)$ denotes the Gamma function, m is the fading parameter, and $\Omega_l = E[|\alpha_{ij}^k(l)|^2]$ is the average power. The powers of the L paths are normalized such that $\sum_{l=0}^{L-1} \Omega_l = 1$. We assume that the time delay τ_l and the average power Ω_l are the same for every transmit-receive link. From (3), the channel frequency response is given by

$$H_{ij}^k(f) = \sum_{l=0}^{L-1} \alpha_{ij}^k(l) \exp(-j2\pi f \tau_l).$$

C. Receiver Processing

The signal received at each receive antenna is a superposition of the N_t transmitted signals corrupted by additive white Gaussian noise. Assume that the receiver perfectly synchronizes to the band switching pattern. The received RF signal at each receive antenna is downconverted to a complex baseband signal, matched to the pulse waveform, and then sampled before passing through an OFDM demodulator. After the OFDM modulator discards the cyclic prefix and performs an N -point FFT, a maximum-likelihood detection is jointly performed across all N_r receive antennas. The choice of prefix length greater than the duration of the channel impulse response, i.e., $T_{CP} \geq \tau_{L-1}$, ensures that the interference between OFDM symbols is eliminated. Effectively, the frequency-selective fading channel decouples into a set of N parallel frequency-nonselective fading channels, whose fading coefficients are equal to the channel frequency response at the center frequency of the subcarriers. Therefore, the received signal at the n th subcarrier at receive antenna j during the k th OFDM symbol duration can be expressed as

$$y_j^k(n) = \sqrt{\frac{E}{N_t}} \sum_{i=1}^{N_t} d_i^k(n) H_{ij}^k(n) + z_j^k(n) \quad (4)$$

where

$$H_{ij}^k(n) = \sum_{l=0}^{L-1} \alpha_{ij}^k(l) \exp[-\mathbf{j}2\pi n\Delta f\tau_l] \quad (5)$$

is the frequency response of the channel at subcarrier n between the i th transmit and the j th receive antenna during the k th OFDM block. In (4), $z_j^k(n)$ represents the noise sample at the n th subcarrier. We model $z_j^k(n)$ as complex Gaussian random variable with zero mean and a two-sided power spectral density of $N_0/2$.

For subsequent performance evaluation, we provide a matrix representation of (4) as follows. Based on the formulation in [23], we rewrite the received signal at receive antenna j in the matrix form as

$$\mathbf{Y}_j = \sqrt{\frac{E}{N_t}} \mathbf{S}_D \mathbf{H}_j + \mathbf{Z}_j \quad (6)$$

where \mathbf{S}_D is a $KN \times KN N_t$ data matrix of a form

$$\mathbf{S}_D = [\mathbf{S}_1 \quad \mathbf{S}_2 \quad \cdots \quad \mathbf{S}_{N_t}] \quad (7)$$

in which \mathbf{S}_i is a $KN \times KN$ diagonal matrix whose main diagonal comprises the information to be sent from transmit antenna i . We format \mathbf{S}_i as

$$\mathbf{S}_i = \text{diag} \left(\left[(\mathbf{d}_i^0)^T (\mathbf{d}_i^1)^T \cdots (\mathbf{d}_i^{K-1})^T \right]^T \right)$$

where $\text{diag}(\mathbf{x})$ is a diagonal matrix with the elements of \mathbf{x} on its main diagonal. The $KN N_t \times 1$ channel vector \mathbf{H}_j is of a form

$$\mathbf{H}_j = [\mathbf{H}_{1j}^T \quad \mathbf{H}_{2j}^T \quad \cdots \quad \mathbf{H}_{N_t j}^T]^T \quad (8)$$

where $\mathbf{H}_{ij} = [H_{ij}^0(0) \cdots H_{ij}^0(N-1) \cdots H_{ij}^{K-1}(0) \cdots H_{ij}^{K-1}(N-1)]^T$. The received signal \mathbf{Y}_j of size $KN N_r \times 1$ is given by $\mathbf{Y}_j = [(\mathbf{y}_j^0)^T (\mathbf{y}_j^1)^T \cdots (\mathbf{y}_j^{K-1})^T]^T$, in which \mathbf{y}_j^k is an $N \times 1$ vector whose n th element is $y_j^k(n)$. The noise vector \mathbf{Z} has the same form as \mathbf{Y} by replacing $y_j^k(n)$ with $z_j^k(n)$.

We assume that the receiver has perfect knowledge of the channel state information, while the transmitter has no channel information. The receiver exploits a maximum likelihood decoder, where the decoding process is jointly performed on N_r receive signal vectors. The decision rule can be stated as

$$\hat{\mathbf{D}} = \arg \min_{\mathbf{D}} \sum_{j=1}^{N_r} \left\| \mathbf{Y}_j - \sqrt{\frac{E}{N_t}} \mathbf{S}_D \mathbf{H}_j \right\|^2.$$

III. PERFORMANCE ANALYSIS

In this section, we first present a general framework to analyze the performance of multiband MIMO coding for UWB communication systems. Then, we derive the average pairwise error probability (PEP) of the proposed system under the Nakagami- m frequency-selective fading channel model. Finally, we quantify the performance criteria in terms of diversity order and coding gain, and determine the maximum achievable diversity advantage for such systems.

Suppose that \mathbf{D} and $\hat{\mathbf{D}}$ are two distinct STF codewords. The PEP, denoted by P_e , is defined as the probability of erroneously decoding the STF codeword $\hat{\mathbf{D}}$ when \mathbf{D} is transmitted. Let \mathbf{S}_D and $\mathbf{S}_{\hat{D}}$ be two data matrices, related to the STF codewords \mathbf{D}

and $\hat{\mathbf{D}}$, respectively. Following the computation steps as in [36], the PEP conditioned on the channel matrix is given by

$$P_e | \mathbf{H}_j = Q \left(\sqrt{\frac{\rho}{2N_t} \sum_{j=1}^{N_r} \|(\mathbf{S}_D - \mathbf{S}_{\hat{D}}) \mathbf{H}_j\|^2} \right) \quad (9)$$

where $\rho = E/N_0$ is the average signal-to-noise ratio (SNR) at each receive antenna, and $Q(x)$ is the Gaussian error function, $Q(x) = (1/\sqrt{2\pi}) \int_x^\infty \exp(-s^2/2) ds$. The average PEP can be obtained by calculating the expected value of the conditional PEP with respect to the distribution of $\gamma \triangleq \sum_{j=1}^{N_r} \|(\mathbf{S}_D - \mathbf{S}_{\hat{D}}) \mathbf{H}_j\|^2$, i.e.,

$$P_e = \int_0^\infty Q \left(\sqrt{\frac{\rho}{2N_t} s} \right) p_\gamma(s) ds \quad (10)$$

where $p_\gamma(s)$ represents the pdf of γ .

For convenience, let us denote an $N_t N_r L K \times 1$ channel vector

$$\mathbf{a} = [\mathbf{a}_1^T, \mathbf{a}_2^T \cdots \mathbf{a}_{N_r}^T]^T$$

where \mathbf{a}_j contains the multipath gains from all transmit antennas to the j th receive antenna. The $N_t L K \times 1$ vector \mathbf{a}_j is formatted as

$$\mathbf{a}_j = \left[(\mathbf{a}_{1j}^0)^T \cdots (\mathbf{a}_{N_t j}^0)^T \cdots (\mathbf{a}_{1j}^{K-1})^T \cdots (\mathbf{a}_{N_t j}^{K-1})^T \right]^T \quad (11)$$

in which

$$\mathbf{a}_{ij}^k = [\alpha_{ij}^k(0) \alpha_{ij}^k(1) \cdots \alpha_{ij}^k(L-1)]^T. \quad (12)$$

According to (5) and (11), we can express (8) as

$$\mathbf{H}_j = (\mathbf{I}_{KN_t} \otimes \mathbf{W}) \mathbf{a}_j$$

where \otimes denotes the Kronecker product [34], \mathbf{I}_M represents an $M \times M$ identity matrix, and \mathbf{W} is an $N \times L$ Fourier matrix, defined as

$$\mathbf{W} = \begin{pmatrix} 1 & 1 & \cdots & 1 \\ \omega^{\tau_0} & \omega^{\tau_1} & \cdots & \omega^{\tau_{L-1}} \\ \vdots & \vdots & \ddots & \vdots \\ \omega^{(N-1)\tau_0} & \omega^{(N-1)\tau_1} & \cdots & \omega^{(N-1)\tau_{L-1}} \end{pmatrix}$$

in which $\omega = \exp(-\mathbf{j}2\pi\Delta f)$. As a consequence, γ can be expressed as

$$\gamma = \sum_{j=1}^{N_r} \|(\mathbf{S}_D - \mathbf{S}_{\hat{D}})(\mathbf{I}_{KN_t} \otimes \mathbf{W}) \mathbf{a}_j\|^2. \quad (13)$$

We can see from (13) that the distribution of γ depends on the joint distribution of the multipath gain coefficients, $\alpha_{ij}^k(l)$.

In the sequel, we evaluate the average PEP of multi-antenna multiband UWB systems with $|\alpha_{ij}^k(l)|$ being Nakagami- m distributed. First, we analyze the performance of a system with independent fading. Such assumption allows us to characterize the performances of UWB systems with the diversity and the coding advantages. The performance of independent fading system also provides us a benchmark for subsequent performance comparisons. Then, we investigate the performance of a more realistic system, where the multipath gain coefficients are allowed to be correlated.

A. Independent Fading

Due to the band hopping, the K OFDM symbols in each STF codeword are sent over different subbands. With an ideal band hopping, we assume that the signal transmitted over K different frequency-bands undergo independent fading. We also assume that the path gains $\alpha_{ij}^k(l)$ are independent for different paths and different pairs of transmit and receive antennas, and that each transmit and receive link has the same power delay profile, i.e., $E[|\alpha_{ij}^k(l)|^2] = \Omega_l$. The correlation matrix of \mathbf{a}_j is given by

$$E[\mathbf{a}_j \mathbf{a}_j^H] = \mathbf{I}_{KN_t} \otimes \mathbf{\Omega} \quad (14)$$

where $(\cdot)^H$ denotes conjugate transpose operation, and $\mathbf{\Omega} = \text{diag}(\Omega_0, \Omega_1, \dots, \Omega_{L-1})$ is an $L \times L$ matrix formed from the power of the L paths. Since the matrix $\mathbf{\Omega}$ is diagonal, we can define $\mathbf{\Omega}^{(1/2)} = \text{diag}(\sqrt{\Omega_0}, \sqrt{\Omega_1}, \dots, \sqrt{\Omega_{L-1}})$ such that $\mathbf{\Omega} = \mathbf{\Omega}^{(1/2)} \mathbf{\Omega}^{(1/2)}$. Let $\mathbf{q}_j = (\mathbf{I}_{KN_t} \otimes \mathbf{\Omega}^{(1/2)})^{-1} \mathbf{a}_j$, then it is easy to see that the elements of \mathbf{q}_j are identically independent distributed (iid) Nakagami- m random variables with normalized power $\Omega = 1$. Substitute $\mathbf{a}_j = (\mathbf{I}_{KN_t} \otimes \mathbf{\Omega}^{(1/2)}) \mathbf{q}_j$ into (13), and apply the property of Kronecker product, $(\mathbf{A}_1 \otimes \mathbf{B}_1)(\mathbf{A}_2 \otimes \mathbf{B}_2) = (\mathbf{A}_1 \mathbf{A}_2) \otimes (\mathbf{B}_1 \mathbf{B}_2)$ ([34] p. 251), resulting in

$$\begin{aligned} \gamma &= \sum_{j=1}^{N_r} \left\| (\mathbf{S}_D - \mathbf{S}_{\hat{D}}) (\mathbf{I}_{KN_t} \otimes \mathbf{W} \mathbf{\Omega}^{1/2}) \mathbf{q}_j \right\|^2 \\ &= \sum_{j=1}^{N_r} \mathbf{q}_j^H \mathbf{\Psi} \mathbf{q}_j \end{aligned} \quad (15)$$

where

$$\mathbf{\Psi} = \left(\mathbf{I}_{KN_t} \otimes \mathbf{W} \mathbf{\Omega}^{1/2} \right)^H (\mathbf{S}_D - \mathbf{S}_{\hat{D}})^H (\mathbf{S}_D - \mathbf{S}_{\hat{D}}) \times \left(\mathbf{I}_{KN_t} \otimes \mathbf{W} \mathbf{\Omega}^{1/2} \right). \quad (16)$$

Since $\mathbf{\Psi}$ is a Hermitian matrix of size $KN_t L \times KN_t L$, it can be decomposed into $\mathbf{\Psi} = \mathbf{V} \mathbf{\Lambda} \mathbf{V}^H$, where $\mathbf{V} \triangleq [\mathbf{v}_1 \cdots \mathbf{v}_{KN_t L}]$ is a unitary matrix, and $\mathbf{\Lambda} = \text{diag}\{\lambda_1(\mathbf{\Psi}), \dots, \lambda_{KN_t L}(\mathbf{\Psi})\}$ is a diagonal matrix whose diagonal elements are the eigenvalues of $\mathbf{\Psi}$. After some manipulations, we arrive at

$$\gamma = \sum_{j=1}^{N_r} \sum_{n=1}^{KN_t L} \lambda_n(\mathbf{\Psi}) |\beta_{j,n}|^2 \quad (17)$$

where $\beta_{j,n} \triangleq \mathbf{v}_n^H \mathbf{q}_j$. Since \mathbf{V} is unitary and the components of \mathbf{q}_j are iid, $\{\beta_{j,n}\}$ are independent random variables, whose magnitudes are approximately Nakagami- \tilde{m} distributed with parameter ([35] p. 25)

$$\tilde{m} = \frac{KLN_t m}{KLN_t m - m + 1} \quad (18)$$

and average power $\Omega = 1$. Hence, the pdf of $|\beta_{j,n}|^2$ approximately follows Gamma distribution ([37] p. 24)

$$p_{|\beta_{j,n}|^2}(x) = \frac{1}{\Gamma(\tilde{m})} \left(\frac{\tilde{m}}{\Omega} \right)^{\tilde{m}} x^{\tilde{m}-1} \exp\left(-\frac{\tilde{m}}{\Omega} x\right). \quad (19)$$

Now, the average PEP can be obtained by substituting (17) into (9), and averaging (9) with respect to the distribution of $|\beta_{j,n}|^2$. To this end, we resort to an alternate representation of Q function [37], $Q(x) = (1/\pi) \int_0^{\pi/2} \exp(-x^2/2 \sin^2 \theta) d\theta$ for $x \geq 0$.

This allows us to express (9) in term of the moment generating function (MGF) of γ , denoted by $\phi_\gamma(s)$, as

$$P_e = \frac{1}{\pi} \int_0^{\pi/2} \phi_\gamma \left(-\frac{\rho}{4N_t \sin^2 \theta} \right) d\theta. \quad (20)$$

Due to the fact that $\phi_{|\beta_{j,n}|^2}(s) = (1 - (\Omega/\tilde{m})s)^{-\tilde{m}}$, and $|\beta_{j,n}|^2$ are independent, (20) can be written as

$$P_e = \frac{1}{\pi} \int_0^{\pi/2} \prod_{n=1}^{KLN_t} \left(1 + \frac{\rho}{4N_t \sin^2 \theta} \frac{\Omega}{\tilde{m}} \lambda_n(\mathbf{\Psi}) \right)^{-\tilde{m}N_r} d\theta. \quad (21)$$

At high SNR, the average PEP in (21) can be upper bounded by

$$P_e \leq \prod_{n=1}^{\text{rank}(\mathbf{\Psi})} \left(\frac{\rho}{4N_t} \frac{\Omega}{\tilde{m}} \lambda_n(\mathbf{\Psi}) \right)^{-\tilde{m}N_r}, \quad (22)$$

where $\text{rank}(\mathbf{\Psi})$ and $\{\lambda_n(\mathbf{\Psi})\}_{n=1}^{\text{rank}(\mathbf{\Psi})}$ are the rank and nonzero eigenvalues of matrix $\mathbf{\Psi}$, respectively. In this case, the exponent $\tilde{m}N_r \text{rank}(\mathbf{\Psi})$ determines the slope of the performance curve plotted as a function of SNR, whereas the product $(\Omega/\tilde{m}) (\prod_{n=1}^{\text{rank}(\mathbf{\Psi})} \lambda_n(\mathbf{\Psi}))^{1/\text{rank}(\mathbf{\Psi})}$ displaces the curve. Therefore, the performance merits of STF coded multiband UWB system can be quantified by the minimum values of these two quantities over all pairs of distinct codewords as the diversity gain

$$G_d = \min_{\mathbf{D} \neq \hat{\mathbf{D}}} \tilde{m}N_r \text{rank}(\mathbf{\Psi})$$

and the coding gain

$$G_c = \min_{\mathbf{D} \neq \hat{\mathbf{D}}} \frac{\Omega}{\tilde{m}} \left(\prod_{n=1}^{\text{rank}(\mathbf{\Psi})} \lambda_n(\mathbf{\Psi}) \right)^{\frac{1}{\text{rank}(\mathbf{\Psi})}}.$$

We note that (22) can also be derived from the Chernoff bound of the Q function.

In order to quantify the maximum achievable diversity gain, we calculate the rank of $\mathbf{\Psi}$ as follows. According to (16) and the rank property, we have

$$\text{rank}(\mathbf{\Psi}) = \text{rank}((\mathbf{S}_D - \mathbf{S}_{\hat{D}})(\mathbf{I}_{KN_t} \otimes \mathbf{W} \mathbf{\Omega}^{1/2})).$$

Observe that the size of $\mathbf{S}_D - \mathbf{S}_{\hat{D}}$ is $KN \times KNN_t$, whereas the size of $\mathbf{W} \mathbf{\Omega}^{1/2}$ is $N \times L$. Therefore, the rank of matrix $\mathbf{\Psi}$ becomes $\text{rank}(\mathbf{\Psi}) \leq \min\{KN, KLN_t\}$. Hence, the maximum achievable diversity gain is

$$G_d^{\max} = \min\{\tilde{m}KLN_t N_r, \tilde{m}KNN_r\}. \quad (23)$$

Note that the diversity gain in (23) depends on the parameter \tilde{m} which is close to one for any fading parameter m . Indeed, for multiband UWB-MIMO systems

$$\tilde{m} = \left(1 - \frac{1}{KLN_t} + \frac{1}{KLN_t m} \right)^{-1} \approx 1. \quad (24)$$

For example,

- With $N_t = 2, K = 2, L = 10, m = 2; \tilde{m} = 1.01 \approx 1$.
- With $N_t = 2, K = 2, L = 10, m = 10; \tilde{m} = 1.02 \approx 1$.
- With $N_t = 2, K = 2, L = 20, m = 10; \tilde{m} = 1.01 \approx 1$.

In this case, the maximum achievable diversity gain is well approximated by

$$G_d^{\max} = \min\{KLN_t N_r, KNN_r\}. \quad (25)$$

The result in the analysis above is somewhat surprising since the diversity gain of multiband UWB-MIMO system does not depend on the fading parameter m . The reason behind this is that $\beta_{j,n}$ in (17) is a normalized summation of KLN_t independent Nakagami random variables. When KLN_t is large enough, $\beta_{j,n}$ behaves like a complex Gaussian random variable, and hence the channel is like Rayleigh fading. Since the ultra-wide bandwidth results in a large number of multipath components, the effect of KLN_t on the diversity gain dominates the effect of fading parameter m , and \tilde{m} is close to one for any m . This implies that the diversity advantage does not depend on the severity of the fading. The diversity gain obtained under Nakagami fading with arbitrary m parameter is almost the same as that obtained in Rayleigh fading channels.

We emphasize here the major difference between the use of STF coding in the conventional OFDM systems and in the multiband OFDM systems. For STF coding in the conventional OFDM systems, the symbols are continuously transmitted in the same frequency-band. In this case, the temporal diversity relies on the temporal correlation of the channel, and hence the system performance depends on the time varying nature of the propagation channel [23]. In contrast, the diversity advantage in (25) reveals that by the use of band switching, the STF coded multiband UWB is able to achieve the diversity gain of $\min\{KLN_tN_r, KNN_r\}$, regardless of the channel time-correlation property.

It is worth noting that the proposed theoretical framework incorporates the analysis for ST or SF coded UWB systems as special cases. In case of single-carrier frequency-nonselctive channel, i.e., $N = 1$ and $L = 1$, the performance of STF coded UWB system is similar to that of ST coded UWB system. In case of $K = 1$, i.e., when the coding is performed over one OFDM block, the STF coded UWB system performance is the same as that of SF coded scheme. The maximum achievable diversity reduces to $\min\{LN_tN_r, NN_r\}$. This reveals that as long as the K OFDM symbols are sent on different frequency-bands, coding across K OFDM blocks can offer the diversity advantage of K times larger than that from SF coding approach.

B. Correlated Fading

In this section, we investigate the performance of STF coded multiband UWB systems in correlated fading scenarios. From (13), we know that γ can be expressed as

$$\gamma = \mathbf{a}^H \{ \mathbf{I}_{N_r} \otimes [(\mathbf{I}_{KN_t} \otimes \mathbf{W}^H)(\mathbf{S}_D - \mathbf{S}_{\hat{D}})^H (\mathbf{S}_D - \mathbf{S}_{\hat{D}})(\mathbf{I}_{KN_t} \otimes \mathbf{W})] \} \mathbf{a}. \quad (26)$$

To simplify the analysis, we assume that the channel correlation matrix, $\mathbf{R}_A = E[\mathbf{a}\mathbf{a}^H]$ is of full rank. Since \mathbf{R}_A is positive definite Hermitian symmetric, it has a symmetric square root \mathbf{U} such that $\mathbf{R} = \mathbf{U}^H \mathbf{U}$, where \mathbf{U} is also of full rank [34]. Let $\mathbf{q} = \mathbf{U}^{-1} \mathbf{a}$, then it follows that $E[\mathbf{q}\mathbf{q}^H] = \mathbf{I}_{KLN_tN_r}$, i.e., the components of \mathbf{q} are uncorrelated. Substituting $\mathbf{a} = \mathbf{U}\mathbf{q}$ into (26), we have

$$\gamma = \mathbf{q}^H \Phi \mathbf{q} \quad (27)$$

where $\Phi = \mathbf{U}^H \{ \mathbf{I}_{N_r} \otimes [(\mathbf{I}_{KN_t} \otimes \mathbf{W}^H)(\mathbf{S}_D - \mathbf{S}_{\hat{D}})^H (\mathbf{S}_D - \mathbf{S}_{\hat{D}})(\mathbf{I}_{KN_t} \otimes \mathbf{W})] \} \mathbf{U}$. Accordingly, performing an eigenvalue

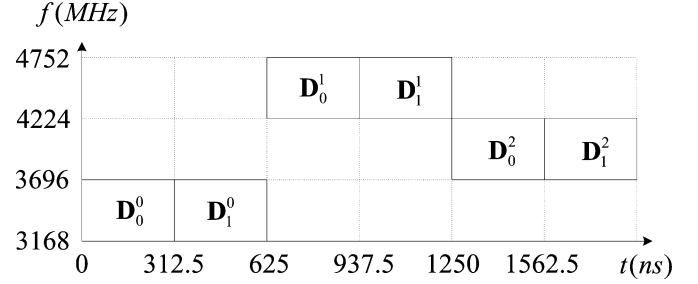


Fig. 3. Time-frequency representation of multiband UWB symbols with $K = 2$ and slow band-hopping rate.

decomposition of the $KLN_tN_r \times KLN_tN_r$ Hermitian symmetric matrix Φ results in $\Phi = \mathbf{V}\mathbf{\Lambda}\mathbf{V}^H$. Therefore, we can express (27) as

$$\gamma = \sum_{n=1}^{KLN_tN_r} \lambda_n(\Phi) |\beta_n|^2, \quad (28)$$

where $\beta_n \triangleq \mathbf{v}_n^H \mathbf{q}$, \mathbf{v}_n s and $\lambda_n(\Phi)$ s are the eigenvectors and the eigenvalues of matrix Φ . From (10) and (28), the PEP can be obtained by averaging the conditional PEP with respect to the joint distribution of $\{|\beta_n|^2\}$, i.e.,

$$P_e = \int_0^\infty \cdots \int_0^\infty Q \left(\sqrt{\frac{\rho}{2N_t} \sum_{n=1}^M \lambda_n(\Phi) s_n} \right) \times p_{|\beta_1|^2 \cdots |\beta_M|^2}(s_1, \dots, s_M) ds_1 \cdots ds_M \quad (29)$$

where $M = KLN_tN_r$. In general, β_n s for different n are not independent, and the closed-form solution for (29) is difficult, if not possible, to determine. In what follows, we will discuss two special cases where the average PEP in (29) can be further simplified.

Special Case 1: Constant Fading: We consider the situation when the MIMO channel stays constant over K OFDM blocks. This corresponds to the case when the modulated OFDM signal is transmitted continually over the same subband for entire K OFDM symbol periods. Fig. 3 illustrates such multiband signal with one of the time-frequency codes in the IEEE 802.15.3a standard proposal [9]. In this example, the STF coding is applied across $K = 2$ OFDM blocks and two OFDM symbols are sent on one subband before the band switching.

In this case, (13) can be re-expressed as

$$\gamma = \sum_{j=1}^{N_r} \|(\mathbf{C}_D - \mathbf{C}_{\hat{D}})(\mathbf{I}_{N_t} \otimes \mathbf{W}) \hat{\mathbf{a}}_j\|^2 \quad (30)$$

where $\mathbf{C}_D = [\mathbf{C}_0^T \mathbf{C}_1^T \cdots \mathbf{C}_{K-1}^T]^T$ is a $KN \times N_tN$ matrix, and $\mathbf{C}_k = [\text{diag}(\mathbf{d}_1^k) \cdots \text{diag}(\mathbf{d}_{N_t}^k)]$. The channel vector $\hat{\mathbf{a}}_j$ of size $LN_t \times 1$ is given by $\hat{\mathbf{a}}_j = [\mathbf{a}_{1,j}^T, \mathbf{a}_{2,j}^T, \dots, \mathbf{a}_{N_t,j}^T]^T$, in which $\mathbf{a}_{i,j}$ is defined in (12). Since the path gains $\mathbf{a}_{i,j}^k$ s are the same for every k , $0 \leq k \leq K-1$, the time superscript index k is omitted to simplify the notations. Following the steps given previously, we can show that the average PEP is of a form similar to (29) with M replaced by LN_tN_r and $\{\lambda_n(\Phi)\}_{n=1}^{LN_tN_r}$ being the eigenvalues of the matrix $\Phi = \hat{\mathbf{U}}^H \{ \mathbf{I}_{N_r} \otimes [(\mathbf{I}_{N_t} \otimes \mathbf{W}^H)(\mathbf{C}_D - \mathbf{C}_{\hat{D}})^H (\mathbf{C}_D - \mathbf{C}_{\hat{D}})(\mathbf{I}_{N_t} \otimes \mathbf{W})] \} \hat{\mathbf{U}}$. Here, $\hat{\mathbf{U}}$ is a symmetric square root of $\hat{\mathbf{R}}_A = E[\hat{\mathbf{a}}\hat{\mathbf{a}}^H]$, in which $\hat{\mathbf{a}} = [\hat{\mathbf{a}}_1^T \hat{\mathbf{a}}_2^T \cdots \hat{\mathbf{a}}_{N_r}^T]^T$.

With a further assumption that the path gains are independent for every transmit-receive link, the average PEP can be obtained in a similar fashion to that derived in Section III-A as

$$P_e \leq \left[\prod_{n=1}^{\text{rank}(\Theta)} \left(\frac{\rho}{4N_t} \frac{\Omega}{\tilde{m}} \lambda_n(\Theta) \right) \right]^{-\tilde{m}N_r} \quad (31)$$

where $\lambda_n(\Theta)$ s are the nonzero eigenvalues of the matrix $\Theta = (\mathbf{I}_{N_t} \otimes \mathbf{W}^H)(\mathbf{C}_D - \mathbf{C}_{\hat{D}})^H(\mathbf{C}_D - \mathbf{C}_{\hat{D}})(\mathbf{I}_{N_t} \otimes \mathbf{W})$. Observe that the maximum rank of $(\mathbf{C}_D - \mathbf{C}_{\hat{D}})(\mathbf{I}_{N_t} \otimes \mathbf{W})$ is $\min\{LN_t, KN\}$. In typical multiband OFDM systems, the number of subcarriers, N is larger than LN_t , hence, the maximum achievable diversity gain of this system is LN_tN_r . Based on this observation, we can conclude that when K OFDM symbols are sent on one subband prior to band switching, coding across K OFDM blocks does not offer any additional diversity advantage compared to the coding scheme within one OFDM block.

Special Case 2: Fading Parameter $m = 1$: With $m = 1$, Nakagami is equivalent to Rayleigh distribution, and the path gain coefficients can be modeled as complex Gaussian random variables. Recall that for Gaussian random variables, uncorrelated implies independent. Thus, $\{|\beta_n|^2\}$ in (28) becomes a set of iid Rayleigh random variables. By using of MGF of γ , the average PEP in (29) is given by

$$P_e = \frac{1}{\pi} \int_0^{\pi/2} \prod_{n=1}^{KLN_tN_r} \left(1 + \frac{\rho}{4N_t \sin^2 \theta} \lambda_n(\Phi) \right)^{-1} d\theta.$$

where Φ is defined in (27). The PEP above can be upper-bounded by

$$P_e \leq \left[\prod_{n=1}^{KLN_tN_r} \left(\frac{\rho}{4N_t} \lambda_n(\Phi) \right) \right]^{-1}$$

at high SNR. Therefore, the diversity gain and the coding gain for this system are defined, respectively, as

$$G_d = \min_{\mathbf{D} \neq \hat{\mathbf{D}}} N_r \text{rank}(\Phi),$$

and

$$G_c = \min_{\mathbf{D} \neq \hat{\mathbf{D}}} \left(\prod_{n=1}^{\text{rank}(\Phi)} \lambda_n(\Phi) \right)^{\frac{1}{\text{rank}(\Phi)}}.$$

IV. SIMULATION RESULTS

To support the theoretical analysis given previously, we perform simulations for multi-antenna multiband UWB systems employing various STF codes. Following the IEEE 802.15.3a standard proposal, our simulated multiband UWB system has $N = 128$ subcarriers and the bandwidth of each subband is $BW = 528$ MHz. Thus, the OFDM symbol is of duration $T_{\text{FFT}} = 128/(528 \text{ MHz}) = 242.42$ ns. After adding the cyclic

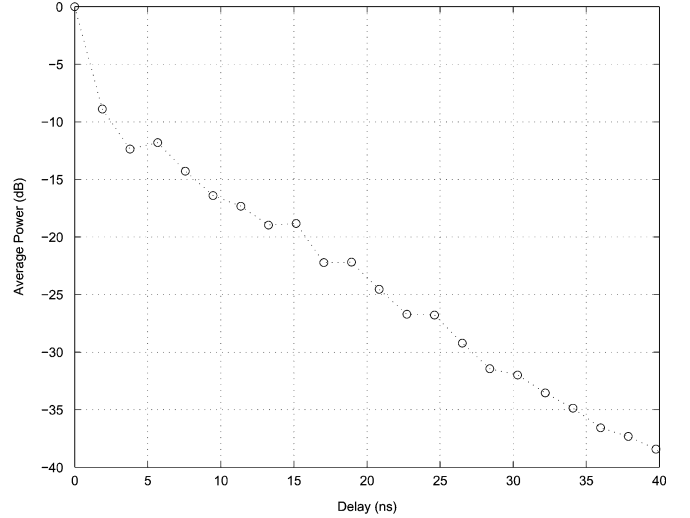


Fig. 4. Power delay profile based on statistical channel model in [38].

prefix of length $T_{\text{CP}} = 60.61$ ns and the guard interval of length $T_{\text{GI}} = 9.47$ ns, the symbol duration becomes $T_{\text{SYM}} = 312.5$ ns.

We simulated the STF coded multiband UWB systems in Nakagami- m fading environment. We employed the stochastic tapped-delay-line channel model in (3), where the path amplitudes $|\alpha_{ij}^k(l)|$ are Nakagami- m distributed and the phases $\angle \alpha_{ij}^k(l)$ are chosen uniformly from $[0, 2\pi)$. The path gain coefficients $\alpha_{ij}^k(l)$ for different i, j , and l are generated independently. The power delay profile, used to specify the path delays τ_l s and powers Ω_l s, follows the statistical model in [38], which is based on an extensive propagation study in residential environments. Fig. 4 shows the power delay profile of the simulated channel. Note that in our simulations, we normalize the total average power of the L paths to unity, i.e., $\sum_{l=0}^{L-1} \Omega_l = 1$.

In our simulations, the STF codeword $\mathbf{D} = [\mathbf{D}_0^T \mathbf{D}_1^T \cdots \mathbf{D}_{K-1}^T]^T$ in (1) is further simplified as

$$\mathbf{D}_k = \begin{bmatrix} \mathbf{G}_{k,1}^T & \mathbf{G}_{k,2}^T & \cdots & \mathbf{G}_{k,P}^T & \mathbf{0}_{(N-P\Upsilon N_t) \times N_t}^T \end{bmatrix}$$

in which Υ is a fixed integer ($\Upsilon \in \{1, 2, \dots, L\}$), $P = \lfloor N/(\Upsilon N_t) \rfloor$, and $\mathbf{0}_{m \times n}$ stands for an $m \times n$ all-zero matrix. The code matrix $\mathbf{G}_{k,p}$ for $p = 1, 2, \dots, P$ and $k = 0, 1, \dots, K-1$ is of size $\Upsilon N_t \times N_t$. The code matrices $\{\mathbf{G}_{k,p}\}_{k=0}^{K-1}$ for each p are jointly designed, whereas the matrices $\mathbf{G}_{k,p}$ and $\mathbf{G}_{k',p'}$ with $p \neq p'$ are designed independently. Such code structures are able to provide the maximum achievable diversity, while enable low computational complexity [23].

Let us consider a system with two transmit antennas. Based on the repetition STF code in [23], $\mathbf{G}_{k,p}$ is given by

$$\mathbf{G}_{k,p} = (\mathbf{I}_{N_t} \otimes \mathbf{1}_{\Upsilon \times 1}) \begin{pmatrix} x_{p,1} & x_{p,2} \\ -x_{p,2}^* & x_{p,1}^* \end{pmatrix}$$

where $\mathbf{1}_{m \times n}$ denotes an $m \times n$ all-one matrix, and $x_{p,i}$ s are selected from BPSK or QPSK constellations. Note that $\mathbf{G}_{k,p}$ is

the same for all k s. We also exploit a full-rate STF code [23], in which $\mathbf{G}_{k,p}$ is

$$\mathbf{G}_{k,p} = \sqrt{N_t} \begin{pmatrix} \mathbf{x}_{p,1}^k & \mathbf{0}_{\Upsilon \times 1} \\ \mathbf{0}_{\Upsilon \times 1} & \mathbf{x}_{p,2}^k \end{pmatrix}. \quad (32)$$

In (32), $\mathbf{x}_{p,i}^k$ is a column vector of length Υ , whose elements are specified as follows. For notation convenience, we omit the subscript p and denote $\mathcal{L} = K\Upsilon N_t$. Let $\mathbf{s} = [s_1 s_2 \dots s_{\mathcal{L}}]$ be a vector of BPSK or QPSK symbols. The $1 \times \mathcal{L}$ matrix $\mathbf{x} \triangleq [(\mathbf{x}_1^0)^T (\mathbf{x}_2^0)^T \dots (\mathbf{x}_1^{K-1})^T (\mathbf{x}_2^{K-1})^T]$ is given by

$$\mathbf{x} = \frac{1}{\sqrt{K}} \mathbf{s} \mathbf{V}(\theta_1, \theta_2, \dots, \theta_{\mathcal{L}})$$

in which \mathbf{V} is a Vandermonde matrix¹ with $\theta_l = \exp(\mathbf{j}(4l - 3)\pi/(2\mathcal{L}))$ for $\mathcal{L} = 2^s (s \geq 1)$ and $\theta_l = \exp(\mathbf{j}(6l - 1)\pi/(3\mathcal{L}))$ for $\mathcal{L} = 2^s \cdot 3^t (s \geq 0, t \geq 1)$ [23]. We note that when $K = 1$, the repetition-coded and full-rate STF codes are reduced to those proposed for SF coding in [18]–[20], respectively. Unless specified otherwise, we apply a random permutation technique [20] so as to reduce the correlation in the channel frequency response among different subcarriers. This permutation strategy allows us to achieve larger coding advantage, and hence improve the system performance. Note that our simulation results are based on the uncoded information. The performance can be further improved by the use of channel coding, such as convolutional and Reed-Solomon codes [9].

In what follows, we present the average bit error rate (BER) curves of multiband UWB systems as functions of the average SNR per bit (E_b/N_0) in dB. In every case, the curves with circles ('o'), crosses ('x') and triangles ('Δ') show the performances of the systems with single transmit and single receive antennas, two transmit and one receive antennas, and two transmit and two receive antennas, respectively.

First, we consider the performance of coding approach over one OFDM block ($K = 1$). We utilize both repetition-coded and full-rate STF codes, each with spectral efficiency of 1 bit/s/Hz (omitting the prefix and guard interval). We use QPSK constellation for the repetition code and BPSK for the full-rate STF code. Both systems achieve the data rate (without channel coding) of $128 \text{ bits}/(312.5 \text{ ns}) = 409.6 \text{ Mbits/s}$. Fig. 5 depicts the performances of the STF coded UWB system with $\Upsilon = 2$. We observe that regardless of particular STF coding scheme, the spatial diversity gained from multi-antenna architecture does improve the system performance significantly. In addition, the performance can be further improved with the choice of STF codes and permutation schemes. In Fig. 6, we compare the performance of multiband UWB system with different frequency diversity orders. Here, we employ the full-rate code with $\Upsilon = 2, 3$, and 4. We can see that by increasing the number of jointly encoded subcarriers, the system performance can be improved. This observation is in accordance with our theoretical result in (22). Therefore, with a properly designed

¹A Vandermonde matrix with variables $\theta_1, \theta_2, \dots, \theta_{\mathcal{L}}$ is a $\mathcal{L} \times \mathcal{L}$ matrix whose l th ($l = 1, 2, \dots, \mathcal{L}$) row is defined as $[\theta_1^{l-1} \theta_2^{l-1} \dots \theta_{\mathcal{L}}^{l-1}]$.

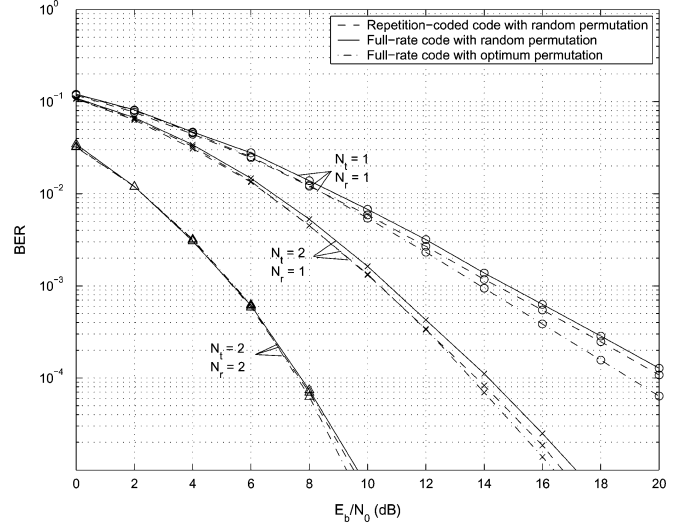


Fig. 5. Performance of multiband UWB with different coding schemes ($K = 1$).

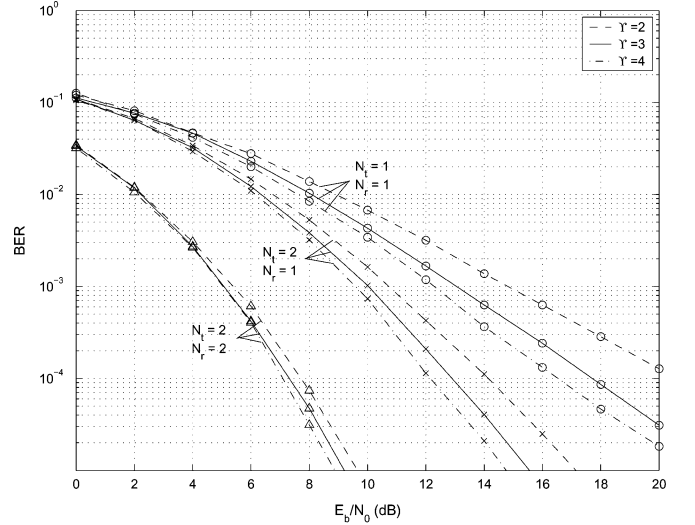


Fig. 6. Performance of multiband UWB with different diversity orders.

STF code, we can effectively exploit both spatial and frequency diversities in UWB environment.

Second, we compare the performances of STF coded multiband UWB system, in which the coding is performed over one and two OFDM blocks ($K = 1, 2$). We consider a scenario when two consecutive OFDM symbols are transmitted over different subbands, for instance, when the multiband signal has a time-frequency representation as in Fig. 2. The performances of the repetition and full-rate STF coded UWB systems with $\Upsilon = 2$ are shown in Fig. 7(a) and (b), respectively. The repetition code is constructed from BPSK constellation for $K = 1$ and QPSK for $K = 2$. Thus, the spectral efficiency of the resulting codes is 0.5 bit/s/Hz. The full-rate STF codes are generated from BPSK constellation for both $K = 1$ and 2, and their spectral efficiency is 1 bit/s/Hz. From both figures, it is apparent that by jointly coding over multiple OFDM blocks, STF coded UWB system has a BER performance curve that is steeper than that of UWB system without jointly encoding, i.e.,

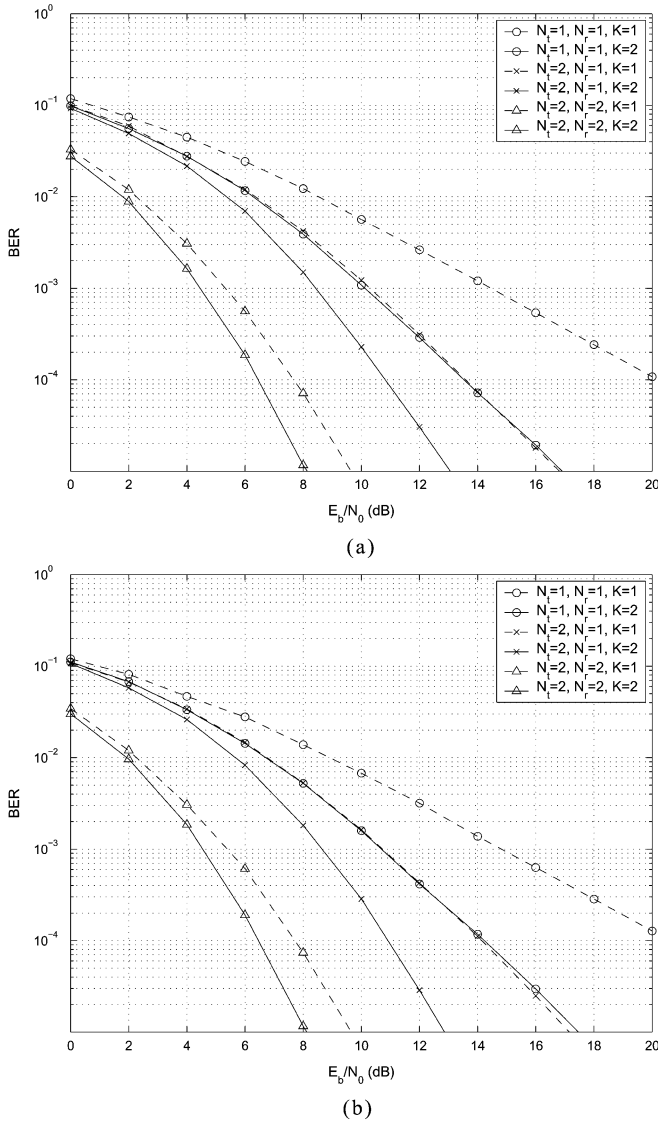


Fig. 7. Performance of multiband UWB with different time spreading factors. (a) Repetition codes, 0.5 bit/s/Hz. (b) Full-rate codes, 1 bit/s/Hz.

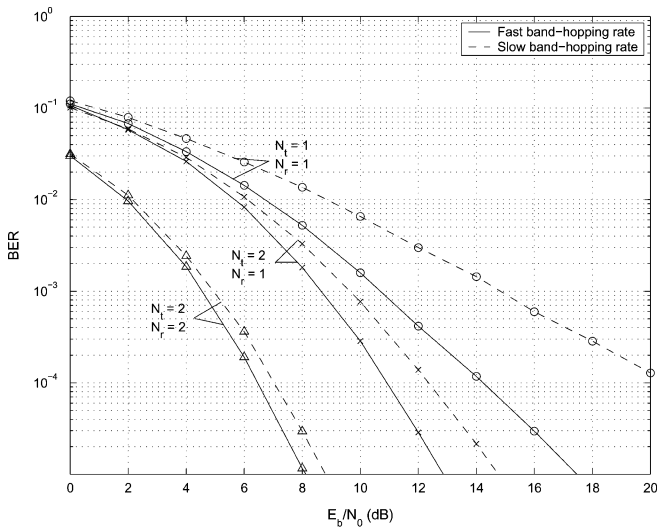


Fig. 8. Performance of multiband UWB with different hopping rates.

the diversity advantage increases with the number of jointly encoded OFDM blocks. Such achieved improvement results from the band hopping rather than the temporal diversity. Hence, by coding across multiple OFDM blocks, the diversity order of STF coded band-hopping UWB increases significantly regardless of the temporal correlation of the channel. This supports our analytical results in the previous section that the diversity order of a STF coded multiband UWB system with fast band-hopping rate is increasing with K .

Finally, we compare the performance of multiband systems with different band-hopping rates. Fig. 8, depicts the performance of full-rate STF coded UWB system with $\Upsilon = 2$ and $K = 2$. Each STF codeword is transmitted during two OFDM block periods. We consider the cases when the two consecutive OFDM symbols are sent on different subband (fast band-hopping rate), and when they are continually transmitted on the same frequency-band (slow band-hopping rate). From Fig. 8, we observe the performance degradation when the band-hopping rate decreases, which corresponds to the results in (22) and (31) that coding over multiple OFDM blocks will offer the additional diversity advantage when the STF coding is applied together with fast band-hopping scheme, i.e., the K OFDM symbols in each STF codeword are transmitted on various frequency-bands.

V. CONCLUSION

In conventional OFDM systems with N_t transmit and N_r receive antennas, STF coding across K OFDM blocks can lead to a maximum achievable diversity order of $T L N_t N_r$, where L is the number of resolvable paths and T is the rank of the temporal correlation matrix of the channel ($T \leq K$). In this paper, we proposed a multiband MIMO coding framework for UWB systems. By a technique of band hopping in combination with jointly coding across spatial, temporal and frequency domains, the proposed scheme is able to exploit all available spatial and multipath diversities, richly inherent in UWB environments. From the theoretical results, we can draw some interesting conclusions as follows. First, the effect of Nakagami fading parameter m on the diversity gain is insignificant, and the diversity advantages obtained in Nakagami- m fading and Rayleigh fading channels are almost the same. Second, the maximum achievable diversity advantage of multiband UWB-MIMO system is $K L N_t N_r$. In contrast to the conventional OFDM, the factor K comes from the band hopping approach, which is regardless of the temporal correlation of the channel. The simulation results showed that the employment of STF coding and band hopping techniques is able to increase the diversity advantage significantly, thereby considerably improving the system performance. In case of single-antenna system, increasing the number of jointly encoded OFDM blocks from one to two yields the performance improvement of 6 dB at a BER of 10^{-4} . By increasing also the number of transmit antennas from one to two, the proposed STF coded multiband UWB system has a total gain of 9 dB at a BER of 10^{-4} .

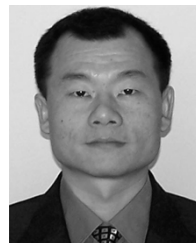
REFERENCES

- [1] *Revision of Part 15 of the Commission's Rules Regarding Ultra-Wideband Transmission Systems, First Report and Order*. Fed. Commun. Comm. Rep., FCC, Washington DC, ET-Docket 98-153.
- [2] R. A. Scholtz, "Multiple access with time-hopping impulse modulation," in *Proc. MILCOM Conf.*, Boston, MA, Oct. 1993, pp. 447–450.
- [3] M. Z. Win and R. A. Scholtz, "Impulse radio: How it works," *IEEE Commun. Lett.*, vol. 2, no. 2, pp. 36–38, Feb. 1998.
- [4] M. L. Welborn, "System considerations for ultra-wideband wireless networks," in *IEEE Radio Wireless Conf.*, Aug. 2001, pp. 5–8.
- [5] J. R. Foerster, "The performance of a direct-sequence spread ultrawideband system in the presence of multipath, narrowband interference, and multiuser interference," in *IEEE Conf. Ultra Wideband Systems Tech.*, May 2002, pp. 87–91.
- [6] N. Boubaker and K. B. Letaief, "Ultra wideband DSSS for multiple access communications using antipodal signaling," in *IEEE Int. Conf. Commun.*, vol. 3, May 2003, pp. 11–15.
- [7] E. Saberinia and A. H. Tewfik, "Pulsed and nonpulsed OFDM ultra wideband wireless personal area networks," in *IEEE Conf. Ultra Wideband Systems Tech.*, Nov. 2003, pp. 275–279.
- [8] J. R. Foerster *et al.*, Intel CFP Presentation for a UWB PHY, Mar. 3, 2003. IEEE P802.15-03/109r1.
- [9] A. Batra *et al.*, "Design of a multiband OFDM system for realistic UWB channel environments," *IEEE Trans. Microw. Theory Tech.*, vol. 52, no. 9, pp. 2123–2138, Sep. 2004.
- [10] J.-C. Guey, M. P. Fitz, M. R. Bell, and W.-Y. Kuo, "Signal design for transmitter diversity wireless communication systems over rayleigh fading channels," *IEEE Trans. Commun.*, vol. 47, pp. 527–537, Apr. 1999.
- [11] V. Tarokh, N. Seshadri, and A. R. Calderbank, "Space-time codes for high data rate wireless communication: Performance criterion and code construction," *IEEE Trans. Inf. Theory*, vol. 44, no. 2, pp. 744–765, Mar. 1998.
- [12] S. Alamouti, "A simple transmit diversity technique for wireless communications," *IEEE J. Sel. Areas Commun.*, vol. 16, no. 8, pp. 1451–1458, Oct. 1998.
- [13] V. Tarokh, H. Jafarkhani, and A. R. Calderbank, "Space-time block codes from orthogonal designs," *IEEE Trans. Inf. Theory*, vol. 45, no. 5, pp. 1456–1467, Jul. 1999.
- [14] B. M. Hochwald and T. L. Marzetta, "Unitary space-time modulation for multiple-antenna communication in Rayleigh flat fading," *IEEE Trans. Inf. Theory*, vol. 46, pp. 543–564, Feb. 2000.
- [15] D. Agrawal, V. Tarokh, A. Naguib, and N. Seshadri, "Space-time coded OFDM for high data-rate wireless communication over wideband channels," in *IEEE Conf. Vehicular Tech.*, vol. 3, 1998, pp. 2232–2236.
- [16] R. Blum, Y. Li, J. Winters, and Q. Yan, "Improved space-time coding for MIMO-OFDM wireless communications," *IEEE Trans. Commun.*, vol. 49, pp. 1873–1878, Nov. 2001.
- [17] H. Bölcskei and A. J. Paulraj, "Space-frequency coded broadband OFDM systems," in *IEEE Wireless Commun. Networking Conf.*, Sep. 2000, pp. 1–6.
- [18] W. Su, Z. Safar, M. Olfat, and K. J. R. Liu, "Obtaining full-diversity space-frequency codes from space-time codes via mapping," *IEEE Trans. Signal Process.*, vol. 51, no. 11, pp. 2905–2916, Nov. 2003.
- [19] W. Su, Z. Safar, and K. J. R. Liu, "Full-rate full-diversity space-frequency codes with optimum coding advantage," *IEEE Trans. Inf. Theory*, vol. 51, no. 1, pp. 229–249, Jan. 2005.
- [20] —, "Systematic design of space-frequency codes with full rate and full diversity," in *IEEE Wireless Commun. Networking Conf.*, vol. 3, Mar. 2004, pp. 1436–1441.
- [21] Y. Gong and K. B. Letaief, "Space-frequency-time coded OFDM for broadband wireless communications," in *IEEE Global Telecommun. Conf.*, vol. 1, Nov. 2001, pp. 519–523.
- [22] A. F. Molisch, M. Z. Win, and J. H. Winters, "Space-time-frequency (STF) coding for MIMO-OFDM systems," *IEEE Commun. Lett.*, vol. 6, no. 9, pp. 370–372, Sep. 2002.
- [23] W. Su, Z. Safar, and K. J. R. Liu, "Towards maximum achievable diversity in space, time and frequency: Performance analysis and code design," *IEEE Trans. Wireless Commun.*, vol. 4, no. 4, pp. 1847–1857, Jul. 2005.
- [24] W. P. Siriwongpairat, M. Olfat, and K. J. R. Liu, "Performance analysis and comparison of time hopping and direct sequence UWB-MIMO systems," in *EURASIP J. Appl. Signal Process. Special Issue on "UWB-State of the Art"*, vol. 2005, Mar. 2005, pp. 328–345.
- [25] —, "On the performance evaluation of TH and DS UWB MIMO systems," in *IEEE Wireless Commun. Networking Conf.*, vol. 3, Mar. 2004, pp. 1800–1805.
- [26] L. Yang and G. B. Giannakis, "Analog space-time coding for multi-antenna ultra-wideband transmissions," *IEEE Trans. Commun.*, vol. 52, no. 3, pp. 507–517, Mar. 2004.
- [27] M. Weisenhorn and W. Hirt, "Performance of binary antipodal signaling over the indoor UWB MIMO channel," in *IEEE Int. Conf. Commun.*, vol. 4, May 2003, pp. 2872–2878.
- [28] D. Cassioli, M. Z. Win, and A. F. Molisch, "The ultra-wide bandwidth indoor channel—From statistical model to simulations," *IEEE J. Sel. Areas Commun.*, vol. 20, pp. 1247–1257, Aug. 2002.
- [29] J. R. Foerster *et al.*, Channel Modeling Sub-Committee Report Final, Nov. 18, 2003. IEEE802.15-02/490.
- [30] H. Hashemi, "Impulse response modeling of indoor radio propagation channels," *IEEE J. Sel. Areas Commun.*, vol. 11, no. 7, pp. 967–978, Sep. 1993.
- [31] Z. Feng and T. Kaiser, "On channel capacity of multi-antenna UWB indoor wireless systems," in *IEEE Int. Symp. Spread Spectrum Techniques and Applications*, Sydney, NSW, Australia, Aug. 30–Sept. 2 2004.
- [32] H. Liu, "Performance of a pulse amplitude and position modulated ultra-wideband system over lognormal fading channels," *IEEE Commun. Lett.*, vol. 7, no. 11, pp. 531–533, Nov. 2003.
- [33] IEEE 802.15WPAN High Rate Alternative PHY Task Group 3a (TG3a) [Online]. Available: www.ieee802.org/15/pub/TG3a.html
- [34] R. A. Horn and C. R. Johnson, *Matrix Analysis*. New York: Cambridge Univ. Press, 1985.
- [35] M. Nakagami, "The m-distribution: A general formula of intensity distribution of rapid fading," in *Statistical Methods in Radio Wave Propagation*, W. G. Hoffman, Ed. Oxford, U.K.: Pergamon, 1960.
- [36] J. G. Proakis, *Digital Communications*, 4th ed. New York: McGraw-Hill, 2001.
- [37] M. K. Simon and M.-S. Alouini, *Digital Communication Over Fading Channels*, 2nd ed, New York: Wiley, 2004.
- [38] S. S. Ghassemzadeh, L. J. Greenstein, T. Sveinsson, and V. Tarokh, "A multipath intensity profile model for residential environments," in *IEEE Wireless Commun. Networking Conf.*, vol. 1, Mar. 2003, pp. 150–155.



W. Pam Siriwongpairat (S'04) received the B.S. degree in electrical engineering from Chulalongkorn University, Bangkok, Thailand, in 1999, and the M.S. and Ph.D. degrees, both in electrical engineering, from the University of Maryland, College Park, in 2001 and 2005, respectively.

She is currently a Postdoctoral Researcher with the Department of Electrical and Computer Engineering and the Institute for Systems Research, University of Maryland, College Park. Her current research interests include signal processing, wireless communications and networking, cross-layer design, and cooperative communications, with particular focus on ultra-wideband communications. Her research contributions encompass space-time and space-frequency coding for multi-antenna ultra-wideband systems.



Weifeng Su (M'03) received the B.S. and Ph.D. degrees in mathematics from Nankai University, Tianjin, China, in 1994 and 1999, respectively. He received the Ph.D. degree in electrical engineering from the University of Delaware, Newark, in 2002.

His research interests span a broad range of areas from signal processing to wireless communications and networking, including space-time coding and modulation for MIMO wireless communications, cooperative communications for wireless networks, and ultrawideband communications. He has published more than 16 journal papers and 24 conference papers in the related areas. From June 2002 to March 2005, he was a Postdoctoral Research Associate with the Department of Electrical and Computer Engineering and the Institute for Systems Research (ISR), University of Maryland, College Park. Currently, he is an Assistant Professor with the Department of Electrical Engineering, State University of New York (SUNY) at Buffalo.

Dr. Su received the Signal Processing and Communications Faculty Award from the University of Delaware in 2002 as an outstanding graduate student in the field of signal processing and communications. He also received the Competitive University Fellowship Award from the University of Delaware in 2001. He won the first prize of the Chinese Olympic Mathematics Competition in 1990.



Masoud Olfat (S'95–M'03) received the B.S. degree in electrical engineering from Sharif University of Technology, Tehran, Iran, in 1993, and the M.S. and Ph.D. degrees both in electrical engineering from University of Maryland, College Park, in 1998 and 2003, respectively.

In February 1998, he joined Odyssey Technology Inc., Laurel, MD, working as a member of technical staff. He consulted at Hermes Technologies Inc., Athens, Greece, in 2001 on the development of IEEE802.11a MAC product. He is currently a senior manager with Nextel Communications Inc., Technology Evaluation and Research Department working on evaluation and development of broadband wireless access technologies, and contributing to WiMAX and IEEE802.16e standard development. His current research interests include coding, power control, multiple antenna schemes, scheduling algorithms for wireless communications systems, handoff in mobile systems, and ultrawideband communications with a special interest in OFDM systems.



K. J. Ray Liu (F'03) received the B.S. degree from the National Taiwan University in 1983 and the Ph.D. degree from the University of California, Los Angeles (UCLA) in 1990, both in electrical engineering.

He is a Professor and Associate Chairman and Director of Graduate Studies and Research of the Electrical and Computer Engineering Department, University of Maryland, College Park. His research contributions encompass broad aspects of wireless communications and networking, information forensics and security, multimedia communications and signal processing, bioinformatics and biomedical imaging, and signal processing algorithms and architectures.

Dr. Liu is the recipient of numerous honors and awards, including Best Paper Awards from the IEEE Signal Processing Society, the IEEE Vehicular Technology Society, and EURASIP; the IEEE Signal Processing Society Distinguished Lecturer; the EURASIP Meritorious Service Award; and the National Science Foundation Young Investigator Award. He also received the Poole and Kent Company Senior Faculty Teaching Award from the A. James Clark School of Engineering and the Invention of the Year Award, both from the University of Maryland. He is Vice-President—Publications and on the Board of Governors of the IEEE Signal Processing Society. He was Editor-in-Chief of the IEEE SIGNAL PROCESSING MAGAZINE and the founding Editor-in-Chief of the *EURASIP Journal on Applied Signal Processing*.